Inhibition and Inactivation of the F_1 Adenosinetriphosphatase from *Bacillus* PS3 by Dequalinium and Activation of the Enzyme by Lauryl Dimethylamine Oxide†

Seung R. Paik, Jean-Michel Jault, and William S. Allison*

Department of Chemistry, University of California at San Diego, La Jolla, California 92093-0601

Received September 1, 1993; Revised Manuscript Received October 20, 1993®

ABSTRACT: The F_1-ATPase from *Bacillus* PS3 (TF_1) hydrolyzes 50 μM ATP in three kinetic phases. An initial burst rapidly decelerates to a partially inhibited, intermediate phase, which, in turn, gradually accelerates to an uninhibited, final steady-state rate. Lauryl dimethylamine oxide (LDAO) stimulates the final rate over 4-fold. The stimulatory effect saturates at about 0.1% LDAO. Under these conditions, the intermediate phase is nearly absent. Dequalinium inhibits TF_1 reversibly in the dark in the presence or absence of LDAO. The apparent affinity of TF_1 for dequalinium increases in the presence of LDAO. Dixon plots of the initial rates of the intermediate phase and the final rates against dequalinium concentration at a series of fixed ATP concentrations in the presence and absence of 0.03% LDAO indicate noncompetitive inhibition in each case. Replots of the slopes of the Dixon plots for the initial rate of the intermediate phase and the final rate against 1/[ATP] reveal apparent K_m values of 770 μM and 144 μM, respectively, when obtained in the absence of LDAO. The apparent K_m values determined from the data obtained in the presence of LDAO for the same phases are 303 μM and 163 μM, respectively. These results suggest that LDAO stimulates ATPase activity either by increasing the affinity of noncatalytic sites for ATP, which promotes release of inhibitory MgADP from a catalytic site, or by directly promoting release of MgADP from the affected catalytic site. Dequalinium retards this process without affecting the affinity of noncatalytic sites for ATP. When irradiated in the presence of dequalinium, TF_1 is rapidly inactivated with an apparent K_d of 12.5 μM in the presence or absence of LDAO. Under both conditions, 90% photoinactivation occurs with incorporation of about 2–2.5 mol of [^{14}C]dequalinium/mol of TF_1. Fractionation of cyanogen bromide–tryptic digests of enzyme photoinactivated with [^{14}C]dequalinium with or without LDAO led to isolation of a labeled peptide containing residues 406–431 of the β subunit in which Phe-420 is derivatized. The results obtained indicate that photoinactivation of TF_1 with dequalinium is accompanied by derivatization of Phe-420 in a single copy of the β subunit and that the residual radioactivity incorporated is the consequence of nonspecific labeling.

The proton-translocating F_oF_1 ATP synthases of energy-transducing membranes couple proton electrochemical gradients produced by electron transport to the condensation of ADP with P_i. The F_o moiety, which is an integral membrane protein complex, mediates transmembrane proton conduction. F_1 is a peripheral membrane complex which can be removed from F_o in soluble form. Isolated F_1 is an ATPase which is composed of five different types of subunits in the stoichiometry $\alpha_3\beta_3\gamma\delta\epsilon$ [for reviews see Penefsky and Cross (1991) and Senior (1988)]. Based on the amino acid sequences of its constituent subunits, the F_1-ATPase from the thermophilic bacterium *Bacillus* PS3 (TF_1)[1] has a molecular weight of 385 000 (Ohta et al., 1988).

The F_1-ATPases contain six nucleotide binding sites. Three of these are potential catalytic sites which appear to be present entirely in β subunits. Three other nucleotide binding sites are present which span α and β subunits (Penefsky & Cross, 1991; Allison et al., 1992). Although it is clear that the hydrolytic activities of CF_1 and MF_1 are modulated by the binding of nucleotides to the latter sites (Milgrom et al., 1990, 1991; Jault & Allison, 1993), the precise physiological function of these sites has not been elucidated, and hence, they are called noncatalytic nucleotide binding sites.

The TF_1-ATPase responds differently to amphiphathic cations which have been shown to be strong inhibitors of MF_1. For instance, rhodamine 6G causes mixed inhibition of MF_1 with a K_i of about 2 μM (Bullough et al., 1989a). In contrast, low concentrations of rhodamine 6G stimulate the ATPase activity of TF_1 (Paik et al., 1993). Maximal stimulation is observed at about 10 μM rhodamine 6G. As the dye concentration is increased above 10 μM, activity decreases with 50% inhibition occurring at about 200 μM rhodamine 6G. In the presence of the neutral detergent LDAO, which by itself activates TF_1 4-fold, the ATPase activity no longer responds biphasically to rhodamine 6G and only inhibition is observed with an $I_{0.5}$ of about 75 μM. Identification of residues modified when MF_1 is inactivated with quinacrine mustard (Bullough et al, 1989b) or photoinactivated with dequalinium [1,1′-(1,10-decanediyl)bis[4-aminoquinolinium]] (Zhuo et al., 1993) indicates that the binding site for inhibitory amphipathic cations in the mitrochondrial enzyme is at an interfacial region near the C-termini of α and β subunits. Inactivation of MF_1 with quinacrine mustard is accompanied by labeling one or any one of the carboxylic acid side chains in the DELSEED segment of the β subunit (Bullough et al., 1989b). In contrast, photoinactivation of MF_1 with dequalinium is accompanied

† This work was supported by U.S. Public Health Service Grant GM 16,974.

* Address correspondence to this author.

® Abstract published in *Advance ACS Abstracts*, December 15, 1993.

[1] Abbreviations: TF_1-ATPase, MF_1-ATPase, and CF_1-ATPase, the F_1 adenosinetriphosphatases from *Bacillus* PS3, bovine heart mitochondria, and spinach chloroplasts, respectively; LDAO, lauryl dimethylamine oxide; HPLC, high-performance liquid chromatography; SDS–PAGE, polyacrylamide gel electrophoresis in the presence of sodium dodecyl sulfate; FSBA, 5′-[*p*-(fluorosulfonyl)benzoyl]adenosine; 8-N_3-FSBA, 5′-[*p*-(fluorosulfonyl)benzoyl]-8-azidoadenosine; OSCP, oligomycin sensitivity conferring protein; HEPES, *N*-(2-hydroxyethyl)piperazine-*N*′-2–ethanesulfonic acid; TPCK, *N*-tosyl-L-phenylalanine chloromethyl ketone.

0006-2960/94/0433-126$04.50/0

by cross-linking Phe-403 or Phe-406 of the α subunit, which are derivatized in mutually exclusive reactions, to a side chain or side chains within residues 440–459 of the β subunit (Zhuo et al., 1993).

Given the different responses of MF_1 and TF_1 to rhodamine 6G (Paik et al., 1993) and chlorpromazine (Bullough et al., 1985), it was of interest to explore the response of the ATPase activity of TF_1 to dequalinium in the presence and absence of LDAO under reversible conditions. When it was discovered that TF_1 and MF_1 respond differently to dequalinium in the absence of light, TF_1 was photoinactivated with [^{14}C]-dequalinium to determine if the two ATPases contain common or different binding sites for the inhibitory amphipathic cation.

MATERIALS AND METHODS

Materials. TF_1 was kindly supplied as a lyophilized powder by Dr. Masasuke Yoshida, which was prepared after exhaustive dialysis of the enzyme against distilled water (Yoshida et al., 1975). The specific activity of the TF_1 used in this study was 9 units/mg when assayed as described below. [^{14}C]Dequalinium with a specific radioactivity of 3 cpm/pmol was synthesized as described previously (Zhuo et al., 1993). Enzymes and biochemicals used in assays and dequalinium dichloride were purchased from Sigma. Cyanogen bromide was obtained from Eastman Kodak. Trypsin treated with TPCK was purchased from Worthington. LDAO (30% aqueous solution) was purchased from Calbiochem. HPLC solvents were obtained from Fisher. Reagents for gel electrophoresis were purchased from Bio-Rad.

Analytical Methods. Protein concentration was determined with bicinchoninic acid (Pierce) as described by Smith et al. (1985). Liquid scintillation counting was performed with Ecoscint from National Diagnostics and a Tm Analytic 6895 counter to detect ^{14}C. Automatic Edman degradations were performed with an Applied Biosystems 470 sequenator. Peptide separations by HPLC were conducted with an Altex Model 332 gradient liquid chromatograph equipped with an LKB 2151 variable-wavelength detector and a Hewlett-Packard integrating chart recorder. The HPLC columns used were C_4 and phenyl reversed phase (Brownlee, 22 cm × 0.46 cm, 7 μm particle size), SCX cation exchange (Rainin, 10 cm × 0.78 cm, 5–12 μm particle size), and TSK G2000$_{SW}$ gel permeation (60 cm × 0.70 cm). Separation of cyanogen bromide fragments by discontinuous polyacrylamide gel electrophoresis in the presence of sodium dodecyl sulfate was performed according to Schägger and Von Jagow (1987).

ATPase activity was determined spectrophotometrically by coupling NADH oxidation with lactate dehydrogenase to pyruvate released from the phosphoenolpyruvate/pyruvate kinase system used to regenerate ATP (Pullman et al., 1960). For assays at saturated ATP, reaction mixtures contained 2 mM ATP, 3 mM $MgCl_2$, 30 mM KCl, 4 mM phosphoenolpyruvate, 10 units/mL lactate dehydrogenase, and 20 units/mL pyruvate kinase in 50 mM Tris-H_2SO_4, pH 8.0. For steady-state kinetic analyses at variable ATP concentrations, $MgCl_2$ was 1 mM in excess of the ATP concentrations. To observe an initial burst during hydrolysis of 50 μM ATP, rates were recorded within 3–5 s of mixing with the aid of a hand-held Bio-Vortexer mixer, Model 1083-MC (Biospec Products). After 10–20 μL of enzyme was loaded onto a notch cut at the distal end of a 5- × 0.2-cm polypropylene stirring rod mounted in the mixer, stirring was initiated as the rod was immersed into the spectrophotometer cuvette. Stirring was continued for about 2 s, at which time the cell compartment of the spectrophotometer (Zeiss M4-QII) was closed and recording was initiated.

Scheme 1: Outline of the Procedure Used To Purify Cyanogen Bromide–Tryptic Peptides Derived from TF_1 Inactivated with [^{14}C]Dequalinium in the Presence of LDAO.

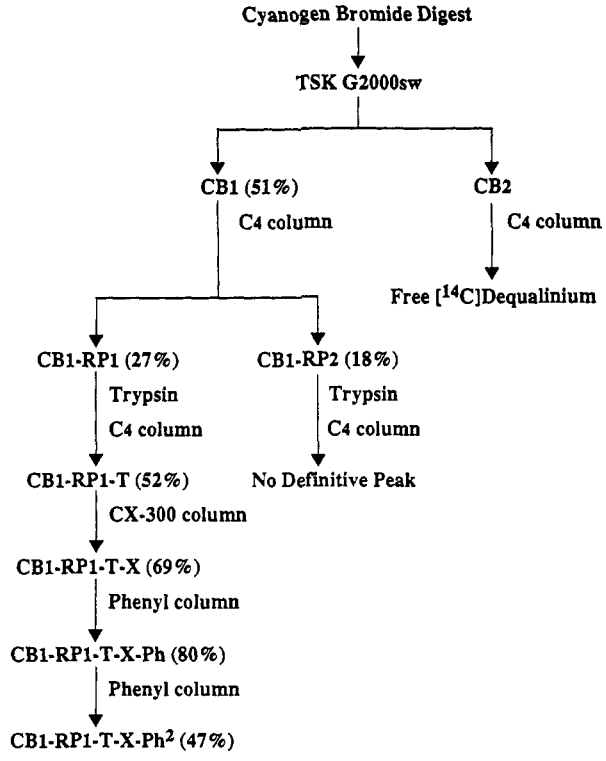

Photoinactivation of TF_1 with [^{14}C]Dequalinium and Generation of Labeled CNBr–Tryptic Fragments from Inactivated Enzyme. Photoinactivations were performed at 23 °C in a Rayonet RMR-400 photochemical reactor with a lamp emitting maximally at 350 nm. The reaction mixtures contained 1 mg/mL TF_1 in 50 mM sodium pyrophosphate, pH 8.0, containing 3 mM $MgSO_4$, 5 mM β-mercaptoethanol, and 13 μM [^{14}C]dequalinium. TF_1, 25 mg in the presence and 15 mg in the absence of 0.03% LDAO, was irradiated with [^{14}C]dequalinium for 4 h to give 81% and 76% inactivation, respectively. Solid ammonium sulfate was added to 75% saturation and the samples were then incubated at 4 °C for 30 min before the protein precipitates were collected by centrifugation. The protein precipitates were dissolved in 2 mL of 6 M guanidinium chloride, pH 7.0, and incubated at room temperature for 16 h. These solutions were dialyzed against 1 L of deionized water at 23 °C for 1 h with one change. This precipitated the protein, which was collected by centrifugation. The denatured protein was dissolved in 2 mL of 70% formic acid, and 30 mg of cyanogen bromide was added/mg of protein present. The resulting solutions were stirred continuously for 16 h at 23 °C. Each reaction mixture was submitted to high-performance gel-permeation chromatography in 0.5-mL aliquots on a TSK G2000$_{SW}$ column which was equilibrated and eluted with 30% formic acid at a flow rate of 0.5 mL/min. This column separated peptide bound radioactivity from free [^{14}C]dequalinium. The fractions containing radioactive peptides resolved from all aliquots of the reaction mixture were combined, concentrated under vacuum in a SpeedVac, and submitted to the fractionation procedure outlined in Scheme 1.

RESULTS

Effects of 0.03% LDAO on Reversible Inhibition of TF_1-ATPase by Dequalinium. Figure 1 illustrates that TF_1

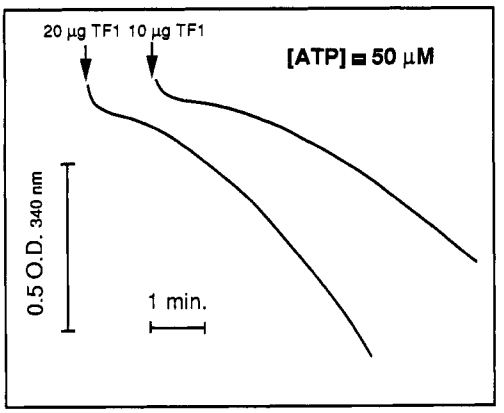

FIGURE 1: TF_1 hydrolyzes ATP in three kinetic phases. The assay mixtures contained 4 mM phosphoenolpyruvate, 30 mM KCl, 0.4 mM NADH, 110 μg/mL lactate dehydrogenase, 210 μg/mL pyruvate kinase, 50 μM ATP, and 1.05 mM $MgCl_2$ in 50 mM HEPES/KOH, pH 8.0. The reactions were initiated with 10 or 20 μL of 1 mg/mL TF_1 which was added with the aid of a hand-held mixer as described under Materials and Methods.

hydrolyzes 50 μM ATP in three distinct kinetic phases. An initial burst rapidly decelerates to a slow intermediate phase which, in turn, gradually accelerates to the final rate. The time required for the transition from the intermediate phase to the final rate decreases as the substrate concentration increases (data not shown). Since the initial burst lasts less than 30 s and special mixing must be employed to observe this phase, the remainder of the rate measurements described were initiated 30 s after mixing and include only the intermediate and final steady-state phases of ATP hydrolysis.

The neutral detergent LDAO stimulates the final steady-state rate of hydrolysis of 2 mM ATP catalyzed by TF_1 (Paik et al., 1993). This effect saturates at about 0.1% LDAO where 4-fold stimulation is observed. This is illustrated in the inset of Figure 2. The intermediate phase is nearly absent when maximal stimulation by LDAO is observed (see Figure 4, traces a and b). Dequalinium is a reversible inhibitor of TF_1 in the dark. Figure 2 shows that 0.03% LDAO increases the apparent affinity of TF_1 to reversible inhibition by dequalinium when the final steady-state rate is monitored during hydrolysis of 2 mM ATP. The $I_{0.5}$ value for inhibition by dequalinium is about 50 μM in the absence of the detergent, whereas it is about 24 μM in the presence of the detergent. To avoid possible complications caused by detergent micelles, 0.03% LDAO was used in the experiments described unless stated otherwise. The critical micelle concentration of LDAO is about 0.05% or 2.2 mM (Helenius et al., 1979).

Figure 3 illustrates that the lag associated with the intermediate phase is extended considerably and the final steady-state rate is inhibited when TF_1 hydrolyzes 200 μM ATP in the presence of increasing concentrations of dequalinium. The effect of increasing concentrations of LDAO on the hydrolysis of 50 μM ATP in the presence of a fixed concentration of 18 μM dequalinium is illustrated in Figure 4, traces c–h. Under these conditions, LDAO shortens the intermediate phase and accelerates the final steady-state rate. However, the final steady-state rate, with respect to controls not containing inhibitor, is inhibited to a greater extent by dequalinium in the presence of LDAO. In the absence of LDAO, the ratio of the final rate in trace c of Figure 4 for inhibited enzyme over that in trace a for uninhibited enzyme is 0.90, whereas the ratio of the final rate in trace e for inhibited enzyme over that in trace b for uninhibited enzyme, which were obtained in the presence of 0.03% LDAO, is 0.32. This

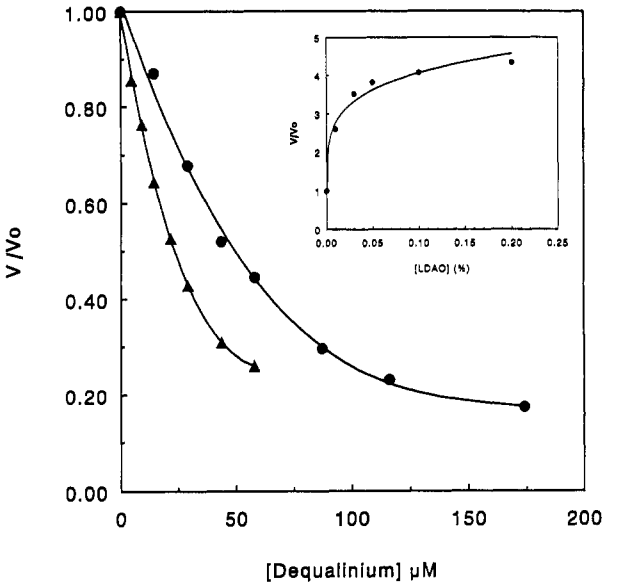

FIGURE 2: Reversible inhibition of TF_1 by increasing concentrations of dequalinium in the presence and absence of 0.03% LDAO. The final steady-state rates were determined as described under Materials and Methods. The final steady-state rates at the dequalinium concentrations indicated (V) are plotted relative to the final steady-state rates determined in the absence of dequalinium (V_0). Each assay mixture contained 5 μg of TF_1. The symbols represent (●) minus LDAO and (▲) plus LDAO. Inset: The effect of LDAO concentration on stimulation of TF_1 in the absence of dequalinium is illustrated.

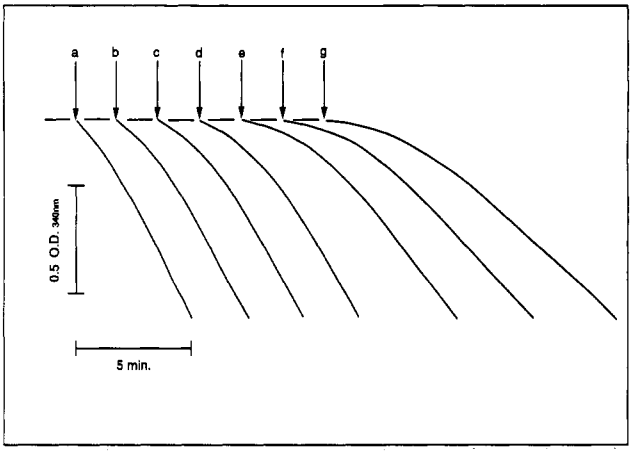

FIGURE 3: Effect of increasing dequalinium concentration on the transition of the intermediate to the final steady-state phase during hydrolysis of 200 μM ATP by TF_1. The assay medium was the same as described under Materials and Methods except that 200 μM ATP and 1.2 mM $MgCl_2$ were employed. The concentrations of dequalinium tested were as follows: trace a, none; trace b, 5.8 μM; trace c, 11.6 μM; trace d, 23.2 μM; trace e, 34.8 μM; trace f, 46.4 μM; and trace g, 58 μM.

comparison also illustrates that LDAO increases the apparent affinity of TF_1 for dequalinium.

Dixon plots constructed from the initial rates of the intermediate phase or the final steady-state rate at varying dequalinium concentrations at a series of fixed ATP concentrations in the presence or absence of 0.03% LDAO showed noncompetitive inhibition in each case. The apparent K_i values obtained in the absence of LDAO were 6.5 μM and 45 μM, respectively, for the initial rate of the intermediate phase and the final steady-state rate. In the presence of 0.03% LDAO, the apparent K_i values were 3.7 μM and 14 μM, respectively, for the initial rate of the intermediate phase and the final steady-state rate. Replots of the slopes of the Dixon plots

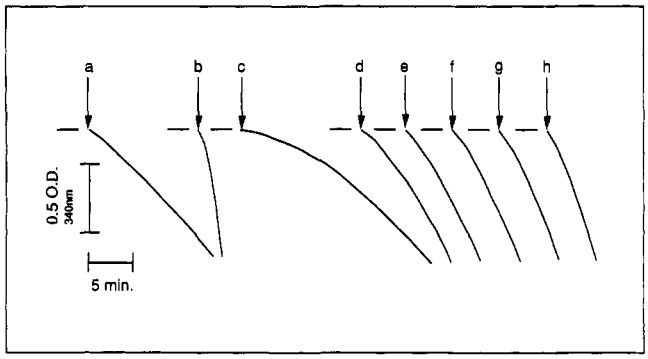

FIGURE 4: Effects of various LDAO concentrations on inhibition of TF_1 (50 μM ATP) by 18 μM dequalinium. The assay medium was the same as described under Materials and Methods except that 50 μM ATP and 1.05 mM $MgCl_2$ were employed. Each assay mixture contained 18 μM dequalinium except for traces a and b. The LDAO concentrations were as follows: trace a, none; trace b, 0.2%; trace c, none; trace d, 0.01%; trace e, 0.03%; trace f, 0.05%; trace g, 0.1%; and trace h, 0.2%.

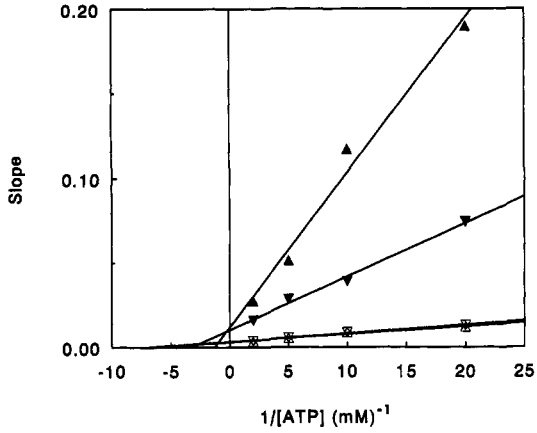

FIGURE 5: Replots of the slopes of Dixon plots of the initial rates of the intermediate and final steady-state phases obtained at increasing concentrations of dequalinium in the presence and absence of LDAO. ATPase activities were determined in the presence of increasing concentration of dequalinium at the fixed ATP concentrations of 50, 100, 200, and 500 μM in the presence and absence of 0.03% LDAO as described under Materials and Methods. The $MgCl_2$ concentration was 1 mM in excess of the ATP concentration. Dixon plots were constructed from the initial rates of the intermediate phase and the final steady-state rates in the absence of LDAO. The initial rates of the intermediate phase were determined from 30 to 50 s after initiating the assays. The final steady-state rates were measured from 4 to 5 min after initiating the assays. The slopes of the lines in the Dixon plots were replotted against the ATP concentration at which they were obtained. Slope replots from initial rates of the intermediate phase are represented by (▼) in the presence and by (▲) in the absence of 0.03% LDAO. Slope replots from the final steady-state rates are represented by (▽) in the presence and by (△) in the absence of 0.03% LDAO.

against the reciprocals of the ATP concentrations at which they were determined are illustrated in Figure 5. The apparent K_m values obtained, which correspond to the initial rate of the intermediate phase and the final steady-state rate in the absence of LDAO, are 770 μM and 144 μM, respectively. The K_m values determined from replots of data obtained for the initial rate of the intermediate phase and the final steady-state rate in the presence of LDAO are 308 μM and 163 μM, respectively. From Lineweaver–Burk plots (data not shown) constructed from rate measurements in the absence of LDAO and dequalinium the following kinetic parameters were obtained: K_{m1} = 124 μM, V_{max1} = 22 s^{-1}; and K_{m2} = 657 μM, V_{max2} = 62 s^{-1}. The values obtained for rate measurements obtained in the presence of 0.2% LDAO but in the absence of dequalinium were K_{m1} = 121 μM, V_{max1} = 37 s^{-1}; and K_{m2} = 255 μM, V_{max2} = 261 s^{-1}.

Photoinactivation of TF_1 with Dequalinium. TF_1 is photoinactivated by dequalinium in a concentration-dependent manner in the presence or absence of 0.03% LDAO. Double-reciprical plots of the pseudo-first-order rate constants for photoinactivation of enzyme against dequalinium concentration revealed an apparent K_d of 12.5 μM in the presence or absence of 0.03% LDAO. Figure 6 illustrates the covalent incorporation of ^{14}C into TF_1 during photoinactivation with [^{14}C]dequalinium in the presence and absence of 0.03% LDAO. In the absence of LDAO, incorporation of ^{14}C was linear at least to 80% inactivation, whereas in the presence of LDAO, deviation from linearity is apparent at 60% inactivation, indicating that the detergent exposes nonspecific reaction sites for dequalinium as inactivation progresses. About 1.9 mol and 2.6 mol of [^{14}C]dequalinium are incorporated/mol on 90% inactivation of TF_1 with [^{14}C]dequalinium in the presence and absence of 0.03% LDAO, respectively.

Derivatization of Phe-β420 Accompanies Photoinactivation of TF_1 with [^{14}C]Dequalinium. Large-scale photoinactivations of TF_1 with [^{14}C]dequalinium were performed in the presence (25 mg) and absence (15 mg) of 0.03% LDAO. Labeling and fractionation procedures for enzyme photoinactivated in the presence or absence of LDAO were similar and led to essentially the same results. Therefore, only the scheme for isolating labeled peptide fragments following inactivation of the enzyme with [^{14}C]dequalinium in the presence of 0.03% LDAO will be outlined. Following 81% photoinactivation of 25 mg of TF_1 with 13 μM [^{14}C]-dequalinium and removal of most of the free [^{14}C]dequalinium, labeled protein was digested with cyanogen bromide as described under Materials and Methods. The resulting digest was submitted to gel-permeation chromatography on a TSK $G2000_{SW}$ column, which removed residual, free [^{14}C]dequalinium from labeled peptides. After removal of free [^{14}C]-dequalinium, it was estimated that 1.9 mol of reagent was incorporated when the enzyme was photoinactivated by 81%. The pooled fractions containing radioactive cyanogen bromide peptides, designated CB_1 in Scheme I, were submitted to reversed-phase HPLC on a C_4 column which resolved a major radioactive peak, CB_1-RP_1, containing 27% of the radioactivity applied to the column and a minor fraction, CB_1-RP_2, containing 18% of the applied radioactivity. After concentration, the materials in the radioactive peaks were digested with trypsin and resubmitted to reversed-phase HPLC on the C_4 column. Whereas 52% of the radioactivity was recovered in a single peak (CB_1-RP_1-T) when the tryptic digest of CB_1-RP_1 was chromatographed, a definitive radioactive peak was not found in the effluent when CB_1-RP_2 was chromatographed. When CB_1-RP_1-T obtained from the second C_4 step was chromatographed on a SCX-300 cation-exchange column, a single radioactive peak eluted that accounted for 69% of the radioactivity applied, designated CB_1-RP_1-T-X in Scheme I. This material was concentrated and submitted to two consecutive HPLC steps on a phenyl column. A steep linear gradient of acetonitrile was used to elute the first column, whereas a series of isocratic steps with small increasing increments of acetonitrile was used to elute the second phenyl column. Comparison of profiles of radioactivity and optical density at 220 nm of the effluents of the second phenyl column indicated that the single radioactive peak, designated CB_1-RP_1-T-X-Ph_2 in Scheme I, was of sufficient purity for amino acid sequence analysis. Based on peptide-bound radioactivity after the TSK G2000 gel-permeation step, the radioactivity

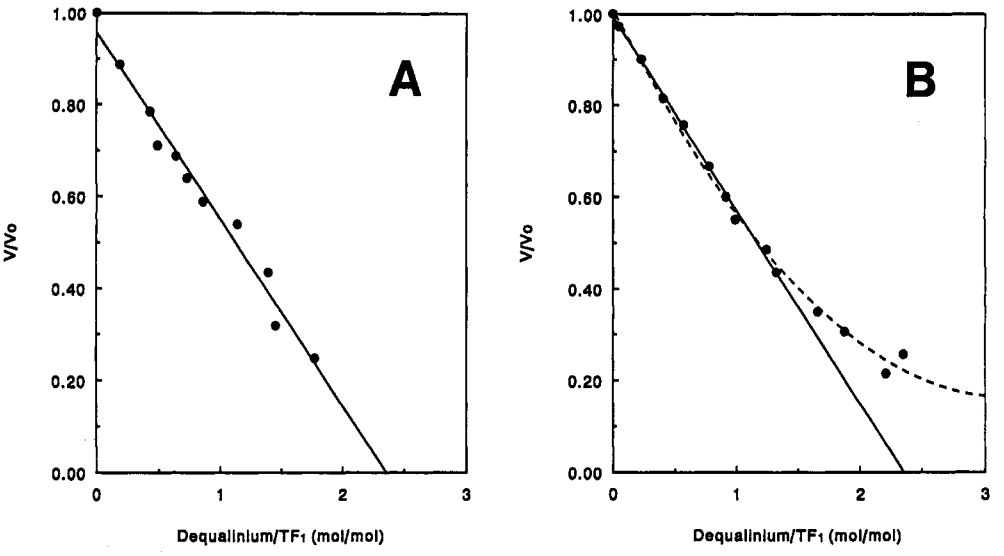

FIGURE 6: Incorporation of ^{14}C during photoinactivation of TF_1 by [^{14}C]dequalinium in the presence (A) and absence (B) of 0.03% LDAO. Photoinactivation was carried out in a Rayonet photochemical reactor at 350 nm with 2.6 μM TF_1 and 13 μM [^{14}C]dequalinium in 50 mM sodium pyrophosphate, pH 8.0, containing 3 mM $MgSO_4$ and 5 mM β-mercaptoethanol added as a radical trap. At intervals after initiating irradiation, 10-μL samples were assayed and 100-μL samples were withdrawn and passed through two consecutive centrifuge columns of Sephadex G-50 (Penefsky, 1977) that were equilibrated with the same buffer. Aliquots of the second eluates were submitted to liquid scintillation counting and protein determination with bicinchoninic acid (Smith et al., 1985). The panels represent (A) photoinactivation in the absence of LDAO and (B) photoinactivation in the presence of LDAO.

Table 1: Edman Degradations of Radioactive CNBr–Tryptic Peptides Isolated after Inactivating TF^1 with [^{14}C]Dequalinium ± LDAO[a]

	plus LDAO					
	sequence 1		sequence 2		LDAO absent	
cycle	residue	pmol	residue	pmol	residue	pmol
1	R	8	I	25	I	26
2	I	25	Q	20	Q	18
3	Q	23	F	19	F	7.4
4	F	(38)[b]	F	(38)[b]	F	12
5	F	21	L	21	L	3.5
6	L	20	S	14	S	1.2
7	S	13	Q	13	Q	1.8
8	Q	13	N	10	N	1.8
9	N	11	F	8.0	F	1.2
10	F	9.4	H	6.5	H	1.0
11	H	8.0	V	4.7	V	0.9
12	V	6.3	A	5.3	A	0.6
13	A	6.8	E	4.6	E	0.6
14	E	6.0	Q	3.5	Q	0.5
15	Q	4.5	–	–		
16	–	–	T	0.9		
17	T	1.0	G	2.5		
18	G	2.5	Q	1.8		
19	Q	1.8	P	1.1		
20	P	1.2	G	1.9		
21	G	2.2	S	1.0		
22	S	11	Y	0.4		
23	Y	0.4	V	0.5		

[a] Sequence according to Ohta et al. (1988) is R-I-Q-F-F-L-S-Q-N-F-H-V-A-E-Q-F*-T-G-Q-P-G-S-Y. [b] This value represents the total Pth-phenylalanine determined in this cycle.

recovered with peptide CB_1-RP_1-T-X-Ph_2 represented 3.6% of the total incorporated during photoinactivation.

Table 1 shows the results of partial amino acid sequence analyses of the radioactive material in CB_1-RP_1-T-X-Ph_2 and the corresponding material obtained after fractionating cyanogen bromide–tryptic digests of TF_1 photoinactivated with [^{14}C]dequalinium in the absence of LDAO. Automatic sequence analysis of the material in CB_1-RP_1-T-X-Ph_2 gave a mixed sequence reflecting incomplete tryptic cleavage between Arg-405 and Ile-406 of the β subunit owing to the consecutive arginine residues at positions 405 and 406. In the cycle corresponding to Phe-420 of the β subunit of TF_1 for both sequences, no Pth-Phe was found, indicating that this is the derivatized residue. The radioactive CNBr–tryptic peptide isolated from TF_1 photoinactivated with [^{14}C]dequalinium in the absence of LDAO was recovered in 8.4% yield. When this was submitted to 14 cycles of automatic Edman degradation, a single sequence was revealed corresponding to residues 406–419 of the β subunit.

The specificity of labeling was monitored by examining large radioactive fragments in a cyanogen bromide digest of MF_1 photoinactivated with [^{14}C]dequalinium. To this end, 50 μg (1000 cpm of ^{14}C) of a cyanogen bromide digest of TF_1 which was photoinactivated with [^{14}C]dequalinium in the absence of LDAO was submitted to SDS–PAGE according to the procedure of Schägger and von Jagow (1987). After electrophoresis, the lane in which the labeled peptide mixture migrated was cut into slices. Figure 7 shows the profile of radioactivity obtained when the slices were digested and submitted to liquid scintillation counting. The major band of radioactivity, which accounted for 28% of the radioactivity applied to the gel, migrated with an M_r of 8.9. The molecular mass calculated for residues 390–469 of the β subunit of TF_1, the cyanogen bromide peptide containing Phe-β420, is 9.0 kDa.

The cyanogen bromide digest submitted to SDS–PAGE was prepared from enzyme which had been inactivated by 73% with [^{14}C]dequalinium. Following removal of excess reagent using two centrifuge columns of Sephadex G-50, precipitation with ammonium sulfate, denaturation with guanidium chloride, and dialysis against distilled water, it was estimated that inactivation was accompanied by incorporation of 2.8 mol of [^{14}C]dequalinium/mol of enzyme. However, when cyanogen bromide digests prepared from TF_1 which was treated similarly prior to digestion were fractionated by gel-permeation HPLC, considerable free [^{14}C]dequalinium was found in the digests as shown in Scheme 1. Therefore, part of the ^{14}C in the cyanogen bromide digest that was submitted to SDS–PAGE probably was present as free [^{14}C]-

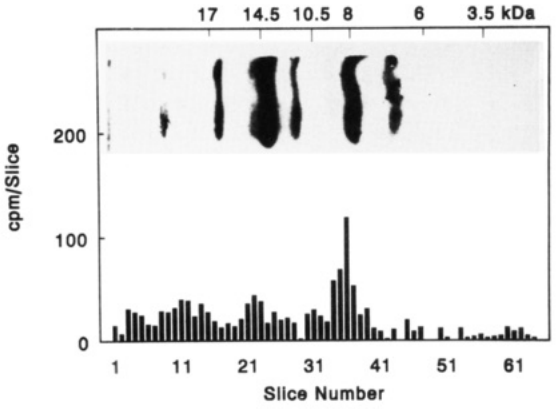

FIGURE 7: Radioactive peptides resolved from a CNBr digest of TF_1 after inactivation with [^{14}C]dequalinium by SDS–PAGE. After inactivation of 3 mg of TF_1 by 73% with 13 μM [^{14}C]dequalinium in the absence of LDAO under the conditions described for a large-scale preparation in Materials and Methods, excess [^{14}C]dequalinium was removed by passing the reaction mixture through two consecutive 5-mL centrifuge columns of Sephadex G-50. Solid ammonium sulfate was added to the second eluate to 75% saturation. The resulting protein precipitate was removed by centrifugation and was dissolved in 1 mL of 6 M guanidinium chloride, pH 4.0. The resulting solution was dialyzed against 1 L of distilled water and the resulting protein precipitate was removed by centrifugation. After the precipitate was dissolved in 70% formic acid, 150 mg of CNBr was added. The reaction mixture was stirred for 16 h at room temperature, at which time excess reagents were removed by lyophilization. The freeze-dried digest was dissolved in 250 μL of 50 mM Tris-HCl containing 12% glycerol (w/v), 4% SDS, and 2% β-mercaptoethanol. A photograph of the gel stained with Coomassic blue is also shown. The masses on the top abscissa represent the positions of migration of markers of known M_r (myoglobin and myoglobin fragments; Sigma MW-SDS-17S) run in a parallel lane.

dequalinium. It is clear from Figure 7 that other large cyanogen bromide peptides are also tagged to a minor extent, probably by nonspecific reaction with the photoactive reagent. In any event, the amount of ^{14}C recovered in the major band of radioactivity illustrated in Figure 7 indicates that on 73% photoinactivation of the enzyme, 0.71 mol of [^{14}C]dequalinium is incorporated onto a specific peptide. Considering these results with the sequences of the isolated, labeled tryptic–cyanogen bromide fragments shown in Table 1 suggests that photoinactivation of the enzyme is associated with derivatization of Phe-420 in a single copy of the β subunit.

DISCUSSION

The kinetic properties of TF_1 resemble those of nucleotide-depleted MF_1 in that it hydrolyzes low concentrations of ATP in three kinetic phases and that it displays apparent negative cooperativity when hydrolyzing 30 μM–2 mM ATP. It has been shown that apparent negative cooperativity exhibited when nucleotide-depleted MF_1 hydrolyzes ATP is associated with slow binding of ATP to noncatalytic sites which promotes dissociation of inhibitory MgADP from a catalytic site (Jault & Allison, 1993). This effect is responsible for an apparent K_m of 440 μM which represents binding of promoter ATP to noncatalytic sites of MF_1 and for the lag associated with the intermediate phase observed during hydrolysis of low concentrations of ATP. The two apparent K_m values obtained in this study for TF_1 from Dixon plots of the initial rate of the intermediate phase (770 μM) and the final steady-state rate (144 μM) in the absence of LDAO are similar to the two K_m values of 124 μM and 657 μM which were obtained from Lineweaver–Burk plots constructed from rate measurements performed in the absence of LDAO. The latter kinetic parameters are similar to the two K_m values of 150 μM and about 1 mM reported earlier for TF_1 by Aloise et al. (1991), which also were obtained from Lineweaver–Burk plots of kinetic data generated in the absence of activators or inhibitors. That the higher apparent K_m value of about 700 μM observed when TF_1 hydrolyzes ATP in the absence of LDAO represents binding of ATP to noncatalytic sites is consistent with the kinetic properties of the $\alpha_3\beta_3\gamma$ complex containing the $D_{261}N$ mutant of the α subunit, which has diminished capacity to bind MgADP (Yohda et al., 1988). Whereas a Lineweaver–Burk plot for ATP hydrolysis catalyzed by the $\alpha_3\beta_3\gamma$ complex containing wild-type α subunit displayed two K_m values of about 20 μM and 1 mM, the complex containing mutant α subunit displayed only a single K_m of about 40 μM.

The observation that LDAO severely diminishes the length of the intermediate phase of ATP hydrolysis by TF_1 and lowers the apparent K_m associated with this phase obtained from Dixon plots suggests that the detergent either increases the affinity of noncatalytic sites for ATP or decreases the affinity of the affected catalytic site for inhibitory MgADP. Dequalinium extends the intermediate phase without affecting the apparent K_m of about 700 μM associated with binding of promoter ATP to noncatalytic sites. This suggests that it might decrease the rate of dissociation of inhibitory MgADP from a catalytic site, either by slowing the response of the affected catalytic site to the binding of ATP to noncatalytic sites or by directly increasing the affinity of the catalytic site for MgADP. Although LDAO and dequalinium have opposite effects on ATPase activity, LDAO increases the affinity of TF_1 for dequalinium. This is reminiscent of the previously reported observation that low concentrations of rhodamine 6G stimulate TF_1 in the absence of LDAO, whereas they inhibit in the presence of the detergent (Paik et al, 1993).

The interactions of TF_1 and MF_1 with dequalinium differ considerably. Photoinactivation of MF_1 with dequalinium cross-links either Phe-403 or Phe-406 of the α subunit, which are derivatized mutually exclusively to a site within residues 440–459 of the β subunit (Zhuo et al., 1993). In contrast, photoinactivation of TF_1 by dequalinium is accompanied by derivatization of Phe-420 of the β subunit. Since the segment containing residues 440–459 of the β subunit of MF_1 correspond to that containing residues 436–455 of the β subunit of TF_1, Phe-β420 of TF_1 is considerably removed, at least in the primary structure, from the site in the β subunit of MF_1 that is derivatized with dequalinium. The position corresponding to Phe-β420 of TF_1 is occupied by phenylalanine in all β subunits which have been sequenced to date. Table 2 illustrates that the region surrounding Phe-β420 of TF_1 is highly conserved. The positions of several amino acid substitutions in the corresponding region of the β subunit of *Escherichia coli* F_1 which affect the activity of the enzyme are indicated in Table 2. It is of particular interest that His-β427 of MF_1 is four residues removed from the conserved phenylalanine corresponding to Phe-β420 of TF_1. Inactivation of MF_1 by FSBA or 8-N_3-FSBA is accompanied by mutually exclusive modification of His-β427 or Tyr-β368, suggesting that both side chains are in the vicinity of the adenine moiety of nucleotides bound to noncatalytic sites (Bullough & Allison, 1986a; Zhuo et al., 1992). Derivatization of His-β427 of MF_1 with 8-N_3-FSBA followed by irradiation cross-links the sulfonylated imidazole side chain of His-427 to Tyr-β345 within the same β subunit. Since Tyr-β345 interacts with the adenine moiety of nucleotides bound to catalytic sites (Garin et al., 1986; Bullough & Allison, 1986b; Cross et al., 1987; Weber et al., 1992), the cross-linking observed suggests that the adenine moieties of nucleotides bound at a catalytic site

Table 2: Sequence Homologies around Phe-β420 of TF_1

			§	
TF_1	406 IQFFL	SQNFHVAEQF	TGQPGSYVPV	430
	† ▽	*	*	
EcF_1	IQRFL	SQPFFVAEVF	TGSPGKYVSL	
			‡	
MF_1	IQRFL	SQPFQVAEVF	TGHLGKLVPL	
CF_1	IERFL	SQPFFVAEVF	TGSPGKYVGL	

§ Modified by [^{14}C]dequalinium in TF_1. † The $R_{398}H$ mutant of EcF_1 is less sensitive to aurovertin (Lee et al., 1989). ▽ A second-site revertant with the $L_{400}Q$ substitution increases the growth yield of an *E. coli* strain with the $S_{174}F$ mutation (Miki et al., 1990). * The double mutant of EcF_1; $P_{403}S$, $G_{415}D$; has impaired activity (Kironde et al., 1989). ‡ Modification of noncatalytic sites in MF_1 by FSBA or 8-N_3-FSBA is accompanied by mutually exclusive modification of H_{427} and Y_{368} (Bullough & Allison, 1986a; Zhuo et al., 1993).

and a noncatalytic site within an interacting α/β pair are within 7–9 Å of each other (Zhuo et al., 1992). If this is indeed the case, Phe-β420 of TF_1 would be near this interaction site, thus supporting the postulate raised earlier from the kinetic analysis that dequalinium inhibits TF_1 by interfering with noncatalytic–catalytic site interactions. The kinetic characteristics of reversible inhibition of the two ATPases by dequalinium also differ. Dequalinium inhibits the final steady-state rate during hydrolysis of 50 μM ATP by MF_1 without producing a disproportionate extension of the intermediate phase (data not shown).

Differences in the subunit compositions of TF_1 and MF_1 may underlie the different responses of the two ATPases to dequalinium and other amphipathic cations. The δ and ϵ subunits of TF_1 are similar in sequence to the corresponding subunits in *E. coli* F_1 (Ohta et al., 1988). The ϵ subunit of *E. coli* F_1 is structurally equivalent to the δ subunit of MF_1 (Walker et al., 1982), whereas the δ subunit of *E. coli* F_1 is equivalent to the oligomycin sensitivity conferring protein (OSCP), which is a component of mitochondrial F_o (Ovchinnikov et al., 1984). The ϵ subunit of MF_1 is unique to mitochondrial F_1-ATPases (Walker et al., 1985). A three-dimensional structure of MF_1 based on X-ray crystallographic analysis of 6.5-Å resolution has recently been reported by Abrahams et al. (1993). Features of the deduced asymmetric structure which are particularly pertinent to this discussion are the following. A 40-Å stem made up of two α helices in a coiled coil extends into a globular sphere which is 110 Å in diameter. A pit, 35 Å deep, is present in the globular portion of the complex next to the stem. Abrahams et al. (1993) postulate that the stem is composed of helical segments of the γ and δ subunits of MF_1 and that the pit might be occupied by either OSCP or the *b* subunit of F_o in the intact, membrane-bound ATP synthase. If the pit in the structure deduced for MF_1 does, indeed, represent the binding site for OSCP and TF_1 is structurally homologous with MF_1, the stem in TF_1 would be composed of the γ and ϵ subunits and the site in TF_1 corresponding to the pit would be filled with the δ subunit. If this were the case, the different interactions of dequalinium with TF_1 and MF_1 could be reconciled by proposing that the binding site for dequalinium in MF_1 is in the pit, whereas the binding site for this inhibitor is elsewhere in TF_1.

Comparison of the effects of LDAO on TF_1 and *E. coli* F_1 deserves comment. Lötscher et al. (1984) originally observed that LDAO stimulates the ATPase activity of *E. coli* F_1. From the observation that cross-linking of the ϵ subunit to the β subunit by a water-soluble carbodiimide did not occur in the presence of LDAO, Lötscher et al. (1984) suggested that activation was caused by release of inhibitory ϵ subunit. Subsequently, Bragg and Hou (1984) showed that ϵ can be cross-linked to β in the presence of LDAO provided that ATP and Mg^{2+} are present. More recently, Dunn et al. (1990) reported that *E. coli* F_1 depleted of the ϵ subunit is stimulated by 140% in the presence of LDAO and concluded that factors in addition to decreasing the affinity of the ϵ subunit are associated with activation of the enzyme by the detergent. Members of the laboratory of Dr. Masasuke Yoshida[2] have recently found that the ϵ subunit suppresses the ATPase activity of $\alpha_3\beta_3\gamma$ complex assembled from the subunits of TF_1 by 40%. The effects of LDAO on the activity of the $\alpha_3\beta_3\gamma$ complex have yet to be examined.

The results presented here show that LDAO lowers the apparent K_m value of about 700 μM which is associated with the binding of ATP to noncatalytic sites. In contrast, Dunn et al. (1990) reported that very little difference in K_m values were detected on Eadie–Hofstee plots when the steady-state kinetics of *E. coli* F_1 were compared in the presence and absence of 0.1% LDAO. However, in making these comparisons, it must be kept in mind that isolated *E. coli* F_1 usually contains 4–5 mol of endogenous adenine nucleotide/mol (Issartel et al., 1986; Hanada et al., 1989), whereas isolated TF_1 contains none. Therefore, in order to make an appropriate comparison, the effects of LDAO on the steady-state kinetics of *E. coli* F_1 depleted of endogenous nucleotides should be examined.

[2] Personal communication from N. Tanaka, S. Matsui, and M. Yoshida, Tokyo Institute of Technology.

ACKNOWLEDGMENT

We thank James A. Register for his assistance in performing gel electrophoresis experiments.

REFERENCES

Abrahams, J. P., Lutter, R., Todd, R. J., van Raaij, M. J., Leslie, A. G. W., & Walker, J. E. (1993) *EMBO J. 12*, 1775–1780.
Allison, W. S., Jault, J.-M., Paik, S. R., & Zhuo, S. (1992) *J. Bioenerg. Biomemb. 24*, 469–477.
Aloise, P., Kagawa, Y., & Coleman, P. S. (1991) *J. Biol. Chem. 266*, 10368–10376.
Bullough, D. A., & Allison, W. S. (1986a) *J. Biol. Chem. 261*, 5722–5730.
Bullough, D. A. & Allison, W. S. (1986b) *J. Biol. Chem. 261*, 14171–14711.
Bullough, D. A., Kwan, M., Laikind, P. K., Yoshida, M., & Allison, W. S. (1985) *Arch. Biochem. Biophys. 236*, 567–575.
Bullough, D. A., Ceccarelli, E. A., Roise, D., & Allison, W. S. (1989a) *Biochim. Biophys. Acta 975*, 377–383.
Bullough, D. A., Ceccarelli, E. A., Verburg, J. G., & Allison, W. S. (1989b) *J. Biol. Chem. 264*, 9155–9163.
Dunn, S. D., Tozer, R. G., & Zadorozny, V. D. (1990) *Biochemistry 29*, 4335–4340.
Garin, J., Boulay, F., Issartel, J. P., Lunardi, J., & Vignais, P. V. (1986) *Biochemistry 25*, 4431–4437.
Hanada, H., Noumi, T., Maeda, M., & Futai, M. (1989) *FEBS Lett. 257*, 465–467.
Helenius, A., McCaslin, D. R., Fries, E., & Tanford, C. (1979) *Methods Enzymol. 56*, 734–749.
Issartel, J.-P., Lunardi, J., & Vignais, P. V. (1986) *J. Biol. Chem. 261*, 895–901.
Jault, J.-M., & Allison, W. S. (1993) *J. Biol. Chem. 268*, 1558–1566.
Kironde, F. A. S., Parsonage, D., & Senior, A. E. (1989) *Biochem. J. 259*, 421–426.
Lee, R. S.-F., Pagan, J., Satre, M., Vignais, P. V., & Senior, A. E. (1989) *FEBS Lett. 253*, 269–272.

Lötscher, H.-R., deJong, C., & Capaldi, R. A. (1984) *Biochemistry 23*, 4140–4143.
Miki, J., Fujiwara, K., Tsuda, M., Tsuchiya, T., & Kanazawa, H. (1990) *J. Biol. Chem. 265*, 21567–21572.
Milgrom, Y. M., Ehler, L. L., & Boyer, P. D. (1990) *J. Biol. Chem. 265*, 18725–18728.
Milgrom, Y. M., Ehler, L. L., & Boyer, P. D. (1991) *J. Biol. Chem. 266*, 11551–11558.
Ohta, S., Yohda, M., Ishuzuka, M., Hirata, H., Hamamoto, T., Otawara-Hamamoto, T., Matsuda, K., & Kagawa, Y. (1988) *Biochim. Biophys. Acta 933*, 141–155.
Ovchinnikov, Y., Modyanov, N. N., Grikevich, V. A., Aldanova, N. A., Kostetsky, P. V., Trubetskaya, O. E., Hundal, T., & Ernster, L. (1984) *FEBS Lett. 175*, 109–112.
Paik, S. R., Yokoyama, K., Yoshida, M., Ohta, T., Kagawa, Y., & Allison, W. S. (1993) *J. Bioenerg. Biomembr.* (in press).
Penefsky, H. S. (1977) *J. Biol. Chem. 252*, 2891–2899.
Penefsky, H. S., & Cross, R. L. (1991) *Adv. Enzymol. Relat. Areas Mol. Biol. 64*, 173–214.
Schägger, H., & von Jagow, G. (1987) *Anal. Biochem. 166*, 368–379.
Senior, A. E. (1988) *Physiol. Rev. 68*, 177–231.
Smith, P. K., Krohn, R. I., Hermanson, G. T., Mallia, A. K., Gartner, F. H., Provenzano, M. D., Fujimoto, E. K., Goeke, N. M., Olson, B. M., & Klenk, D. C. (1985) *Anal. Biochem. 150*, 76–85.
Walker, J. E., Runswick, M. J., & Saraste, M. (1982) *FEBS Lett. 146*, 393–396.
Walker, J. E., Fearnley, L. M., Gay, N. T., Gibson, B. W., Northrop, F. D., Powell, S. J., Runswick, M. J., Saraste, M., & Tybulewicz, V. L. J. (1985) *J. Mol. Biol. 184*, 677–701.
Weber, J., Lee, R.S.-F., Grell, E., Wise, J. G., & Senior, A. E. (1992) *J. Biol. Chem. 267*, 1712–1718.
Yohda, M., Ohta, S., Hisabori, T., & Kagawa, Y. (1988) *Biochim. Biophys. Acta 933*, 156–164.
Yoshida, M., Sone, N., Hirata, H., & Kagawa, Y. (1975) *J. Biol. Chem. 252*, 7910–7916.
Zhuo, S., Garrod, S., Miller, P., & Allison, W. S. (1992) *J. Biol. Chem. 267*, 12916–12927.
Zhuo, S., Paik, S. R., Register, J. A., & Allison, W. S. (1993) *Biochemistry 32*, 2219–2227.